Potential of High-Resolution Satellite Imagery for National Mapping Products

Rongxing Li

Abstract

The potential of the upcoming high-resolution (1-m ground resolution) satellite imagery for national mapping products is discussed. An analysis of the capabilities of these high-resolution imaging systems and existing satellite imaging systems for the representation and extraction of elevation information, such as terrain relief displacement and parallaxes, is given. In-track and cross-track stereo mapping techniques using satellite pushbroom CCD linear arrays are described. A photogrammetric processing model considering such geometry is introduced. Based on an error estimation and analysis, it is concluded that, if the strict photogrammetric processing model and ground control points are employed, high-resolution satellite imagery can be used for the generation and update of national mapping products (7.5-minute quadrangles at a map scale of 1:24,000), including Digital Elevation Models (DEM), Digital Orthophoto Quadrants (DOQ), Digital Line Graph (DLG) databases, and Digital Shoreline (DSL) databases.

Introduction

The launch of the new generation of high-resolution (up to 0.82 m or 1 m) commercial Earth imaging satellites in early 1998 and after will mark the start of a new era of space imaging for Earth observations (Fritz, 1996). Among several commercial high-resolution imaging satellites, Early Bird (3-m resolution) and Quick Bird (1-m resolution) of EarthWatch, Incorporated; IKONOS (1-m resolution) of Space Imaging, Inc.; and OrbView-1 (1-, 2-, and 4-m resolution) of The Orbital Sciences Corporation are planned to be launched in late 1997 and 1998[1]. The imagery will maintain dominant spectral advantages demonstrated by lower resolution satellite imaging systems such as Landsat TM and SPOT. More important is that the new generation of high-resolution satellite imagery will provide strong geometric capabilities that have not been available from existing satellite imaging systems. Specific geometric aspects of the imagery that are interesting to the mapping community include, for example, high-resolution, photogrammetric stereo capability, and revisit rate. With one-metre ground resolution, objects appearing in most digital national mapping products, such as Digital Elevation Models (DEM), Digital Orthophoto Quadrants (DOQ), Digital Line Graphs (DLG), and Digital Shorelines (DSL), can be represented in the imagery (USGS, 1997; Ellis, 1987; Lockwood, 1997). Although linear CCD (charge-coupled device) arrays are used in most one-metre resolution imaging systems and require more complicated photogrammetric models, they will for the first time provide horizontal and vertical positions of measured objects in the ground coordinate system at accuracies of several metres. The revisit rate of 1 to 4 days, depending on the particular satellite system and on latitude, makes it possible to map an area frequently without special flight planning and scheduling as required in aerial photogrammetric data acquisition. Stereo models thus formed are valuable for mapping product updating and accurate change detection.

Accurate elevation information is crucial to national mapping products if satellite data are used. The SPOT imaging system has an enhanced resolution of 10 m in the panchromatic band with a cross-track stereo capability only. Elevation accuracies of around 10 m have been achieved with the aid of ground control points (Al-Rousan *et al.*, 1997), which are not sufficient for many mapping products (USGS, 1997). Airborne mapping is currently still the primary technique employed for national mapping because of its advantages such as high accuracy, flexible scheduling, and easy-to-change configurations. Among the new commercial high-resolution satellite imaging systems, the EarlyBird system of EarthWatch, Incorporated has a ground resolution of 3 m in the panchromatic band and captures images frame by frame. The pushbroom imaging technique with one or more linear CCD arrays has been adopted by systems with 1 m resolution. Such a configuration provides a so-called in-track stereo mode where stereo pairs necessary for deriving the horizontal and elevation information of objects can be acquired in quasi real-time or real-time; cross-track stereo requires additional time to allow the satellite to point to the same ground area from a neighboring track. Stereo mapping capabilities of similar airborne imagers and systems mounted on board the Space Shuttles have been demonstrated (Heipke *et al.*, 1996; Fraser *et al.*, 1997). There are four advantages of high-resolution satellites: (1) the highest resolution ever available to the civilian mapping community; (2) extremely long camera focal length, for example, ten metres, for capturing terrain relief information from satellite orbit; (3) fore-, nadir-, and aft-looking linear CCD arrays supplying in-track stereo strips and "pointing" capabilities generating cross-track stereo strips; and (4) a base-height (sensor baseline vs. orbit height) ratio of 0.6 and greater that is similar to aerial photographs. Table 1 gives some selected technical specifications of the high-resolution commercial satellites, which are important for three-dimensional mapping applications (Fritz, 1996). If not specified, parameters used in equations and estimations in the rest of the paper are based on the IKONOS system (Table 2).

This paper gives an analytical assessment of the map-

[1]At the present time (February 1998) Early Bird is on orbit and experiencing difficulties in two-way communications. Efforts are being made by the company to bring the system to its designed status.

Civil and Environmental Engineering and Geodetic Science, The Ohio State University, 470 Hitchcock Hall, 2070 Neil Avenue, Columbus, OH 43210-1275 (li.282@osu.edu).

Photogrammetric Engineering & Remote Sensing, Vol. 64, No. 12, December 1998, pp. 1165–1169.

0099-1112/98/6412–1165$3.00/0

TABLE 1. SOME SELECTED TECHNICAL SPECIFICATIONS FOR THE HIGH-RESOLUTION COMMERCIAL SATELLITE IMAGERY

Item	Technical Data
Ground Resolution	1 to 3 m
Orbit Height	460 to 680 km
Focal Length	Up to 10 m
Image Recording	CCD linear or frame arrays
Stereo Mode	In-track and/or cross-track stereo
Base-Height Ratio	0.6 to 2.0
Ground Swath Width	6 to 36 km
Revisit Rate	1 to 4 days from most of the northern hemisphere

ping potential of high-resolution commercial satellite imagery. Aspects of photogrammetric processing of the imagery are discussed. An estimation of ground accuracies of measured objects from the imagery is given considering various error sources. Technical requirements of U.S. national mapping products, including DEM, DOQ, DLG, and DSL, are compared with the estimated measuring accuracies. Conclusions and recommendations based on the analysis are made for applications of the imagery in national mapping production.

Three-Dimensional Mapping from Satellite Imagery

Presentation of Elevation Information

The photo scale of a vertical aerial photograph (horizontal image plane) is defined as f/H. For example, aerial photographs for national mapping taken by a camera with a focal length of 152 mm at a flying height of 6000 m have a photo scale of approximately 1:40,000. The high-resolution satellite imagery of IKONOS has a photo scale of 1:68,000 (f/H = 10m/680km). On the other hand, the photo scale can also be expressed as a ratio of an image distance over its corresponding ground distance: d_{photo}/d_{ground}. Taking the ground pixel size as d_{ground} = 0.82 m and the photo scale as 1:68,000, the pixel size on the CCD chip is computed as 12 μm. Therefore, the higher the ground resolution, the smaller the ground pixel size and, furthermore, the smaller the pixel size on the chip. This may impose the ultimate limit on the ground resolution. In order to derive elevation, the relevant information must be present in the images in some form. One of them is terrain relief displacement (Figure 1). Assume that an object on the ground has a height of Δh and a distance R from the nadir point of a vertical aerial photograph with a flying height of H. The focal length of the aerial camera is f. The relief displacement d of the object caused by the elevation difference Δh in the aerial photograph can be calculated as (Moffitt and Mikhail, 1980; Wolf, 1983)

TABLE 2. SOME SELECTED TECHNICAL SPECIFICATIONS FOR THE IKONOS SYSTEM

Item	Technical Data
Pixel Size	12μm (panchromatic)
Ground Resolution	0.82 at nadir (panchromatic)
Multispectral Bands	
Blue (4m)	0.45 to 0.52 μm
Green (4m)	0.52 to 0.60 μm
Red (4m)	0.63 to 0.69 μm
Near-Infrared (4m)	0.76 to 0.90 μm
Focal Length	10m
Image Recording	CCD linear arrays (one for IKONOS I)
Orbit Height	680 km
Scene Coverage	11km by 11km
Stereo Mode	In-track and/or cross-track stereo
Base-Height Ratio	1.0 to 2.0
Revisit Rate	3 days

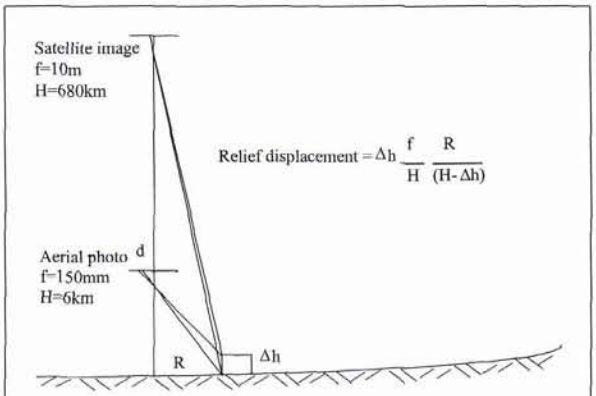

Figure 1. Relief displacement in an aerial photograph and a satellite image.

$$d = \Delta h \frac{f}{H} \frac{R}{(H - \Delta h)}. \quad (1)$$

It is obvious that relief displacement is proportional to the elevation difference Δh. Here, f/H is the photo scale. Small scale photographs are thus less capable of representing relief displacement information. Objects close to the nadir point have small distances R and, therefore, will have small relief displacements. The same elevation difference Δh would produce a larger relief displacement as the object is situated farther away from the nadir point. The terms of Equation (1) are examined for both aerial photography and satellite image cases (Figure 1) where the object height Δh remains the same.

- The flying height increases greatly from aerial photography to satellite imaging. However, a high-resolution camera, for example, IKONOS, has a focal length of 10 m, which makes the second term, f/H (photo scale), comparable to that of an aerial photo scale.
- In the third term $R/(H - \Delta h)$, because H is much greater than Δh, the value of the term decreases rapidly from aerial photography to satellite imaging. Note that the satellite image covers a much larger ground area. In its nadir area, the distance from the nadir point to the object, R, is small, and, therefore, the corresponding terrain relief displacement will be small; in the most imaged area, R is sufficiently large in comparison to H and a ratio of $R/(H - \Delta h)$ becomes close to that of aerial photography.

Generally, it is expected that sufficient terrain relief displacement information will be contained in the high-resolution satellite imagery. Fine topographic variations should be reflected.

In addition to the relief displacement information in single images, parallax, a positional change in the flying direction of an object point in a vertical stereo image pair caused by the imaging platform motion, can be used to derived the elevation or elevation difference (Wolf, 1983): i.e.,

$$p = f \frac{B}{(H - \Delta h)} \quad (2)$$

where p is the parallax of the top point of the object in Figure 1 and B is the baseline distance between the two exposure centers of the camera. In the high-resolution imaging case, the orbit height H is great and makes parallax p small. However, B is great in both cross-track stereo mode and in-track stereo mode because the pointing angle of 30° (Quick Bird) to 45° (IKONOS) yields large baselines by different combinations of fore-, nadir-, and aft-looking strips. The extremely long focal length f makes a further contribution to a greater

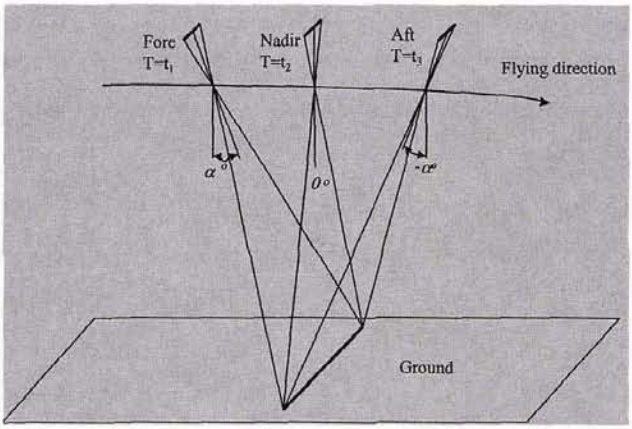

Figure 2. Fore-, nadir-, and aft-looking CCD linear arrays and their look angles.

parallax. The images will have a typical parallax of 85μm to 170μm, or 6 pixels to 12 pixels, which is sufficiently large to be measured and used for deriving elevation information.

Stereo Model Formation

Figure 2 illustrates three CCD linear arrays (fore, nadir, and aft) "looking" at the same ground profile across the track. Note that the three look angles are, for instance, $\alpha°$, 0°, and $-\alpha°$, respectively. Each CCD linear array produces one strip along the track. An object on the ground is usually covered by three image strips. The specific image lines of the strips containing the object are taken at different times. Thus, the in-track stereo mode has three combinations of stereo pairs, namely F-N (fore-nadir), N-A (nadir-aft), and F-A (fore-aft). Baselines are then 271km (Quick Bird) and 680km (IKONOS) for F-N and N-A stereo pairs, and 542km and 1360km, respectively, for F-A pairs.

The base-height ratio is a critical factor for accurate 3D mapping. Aerial photography for national mapping usually has a base-height ratio of 0.6. In the case of high-resolution satellite imaging, the orbit height is, for instance, 680 km. Considering the possible combinations, the base-height ratio of F-N and N-A pairs is 0.6 (Quick Bird) to 1.0 (IKONOS) and, for an F-A pair, is 1.2 to 2.0. This means that the satellite images are able to provide a base-height ratio similar to that of aerial photographs. This partly ensures the quality of the 3D spatial data derived from the imagery.

The pointing capability across track with an angle of 45° (IKONOS) makes it possible to flexibly form cross-track stereo strips. The accuracies of objects derived from the cross-track stereo strips should be similar to those from in-track strips, except that the "side-looking" geometry may produce some refractive effects positive to ground relief along track.

Photogrammetric Modeling

Interior and Exterior Orientation Parameters

To simplify the explanation without losing generality, Figure 3 illustrates the imaging system with fore- and nadir-looking CCD linear arrays (Array I and Array II, respectively). In order to accurately model the imaging geometry, the following interior orientation parameters are defined for each linear array:

- Focal length f;
- Ratio of pixel size δy and δx in the y and x direction, $\delta y/\delta x$;
- Principal point coordinate x_0 (only one image coordinate is needed for a linear array); and
- Lens distortion correction coefficients: p_1, p_2, k_1, k_2, and k_3.

Three lenses can be used, one for each CCD linear array. Or one lens can be used for all three CCD linear arrays. At this time, this information is not available from the imaging companies. The following discussion is based on a three-lens configuration. The above parameters are then for all three CCD linear arrays (fore, nadir, and aft). Each array has its own 2D image coordinate system x_i-O_i-z_i. The linear arrays are subsequently defined in the platform coordinate system X_{pl}-Y_{pl}-Z_{pl}. All coordinate systems are referenced to the ground coordinate system. The two linear arrays have a fixed geometric relationship, i.e., a translation vector O_I-O_{II} or $\Delta\mathbf{r}=(\Delta X, \Delta Y, \Delta Z)_{pl}$ and a rotation matrix $\mathbf{M}_{\Delta pl} = M_\Delta(\Delta\omega, \Delta\phi, \Delta\kappa)_{pl}$ from x_I-O_I-z_I to x_{II}-O_{II}-z_{II} defined in the platform coordinate system. For a system with three linear arrays, there are 36 interior orientation parameters, including eight intra-array parameters for each array and 12 inter-array parameters (two sets of translation and rotation parameters among the three arrays). Here it is assumed that the image coordinate system of Array I is used as the platform coordinate system in order to reduce the parameters involved. Because a laboratory calibration is usually impossible during the lifetime of the satellite, it is recommended that frequent evaluations of the interior orientation parameters be carried out using calibration ranges.

Exterior orientation parameters are used to relate the platform to the ground coordinate system. At any time, the exterior orientation parameters of the platform are coordinates of the origin of the platform coordinate system (X_o, Y_o, Z_o) and rotational angles (ω, ϕ, κ) with respect to the ground coordinate system. The rotation is described by a 3D rotation matrix $\mathbf{M}_{pl}$ which is a function of the rotation angles (Moffitt and Mikhail, 1980). For simplicity mentioned above, the exterior orientation parameters of Array I are identical to the platform: (X_o, Y_o, Z_o) and $\mathbf{M}_{pl}$. Those of Array II are calculated by applying the inter-array parameters (translation and rotation) between Array I and Array II to the exterior orientation parameters of Array I: (X_o, Y_o, Z_o)+ $\mathbf{M}_{pl}\,\mathbf{M}_{\Delta pl}\,\Delta\mathbf{r}$ and $\mathbf{M}_{pl}\,\mathbf{M}_{\Delta pl}$. The exterior orientation parameters of Array III can be computed in the same way.

Photogrammetric Intersection

When the interior and exterior orientation parameters of all lines in the image strips are known, image coordinates of an object in one or more stereo pairs of strips can be measured and used to calculate the ground coordinates of the object.

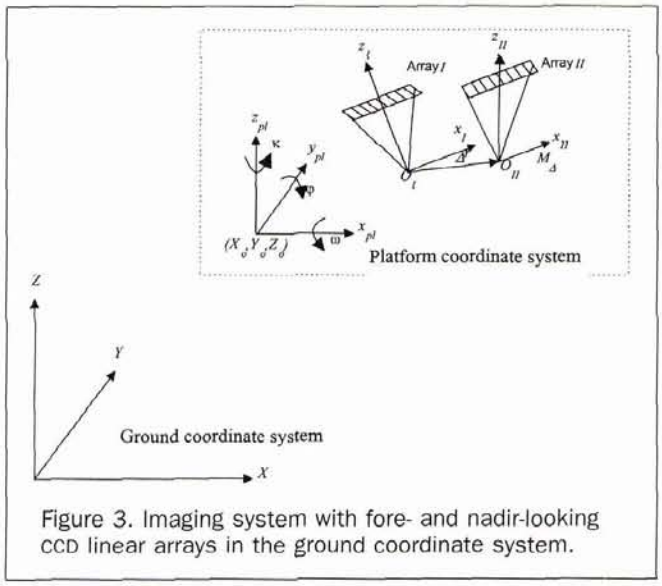

Figure 3. Imaging system with fore- and nadir-looking CCD linear arrays in the ground coordinate system.

This computational procedure is called photogrammetric intersection. Suppose that a stereo line pair consists of an image line of Array I (fore-looking) at time t and an image line of Array II (nadir looking) at time $t+\Delta t$ (Figure 4). Image coordinates, x_I and x_{II}, of a ground point P in both image lines are measured. The ground coordinates of P, or vector $\mathbf{r}$, are to be computed

With the known interior and exterior orientation parameters of $\Delta\mathbf{r}$, $\mathbf{M}_{\Delta pl}$, $(X_o,Y_o,Z_o)_t$, $(X_o,Y_o,Z_o)_{t+\Delta t}$, $\mathbf{M}_{pl,t}$, and $\mathbf{M}_{pl,t+\Delta t}$, the rotation matrices of Array I and Array II are

$$\begin{aligned}\mathbf{M}_{I,t} &= \mathbf{M}_{pl,t} \\ \mathbf{M}_{II,t+\Delta t} &= \mathbf{M}_{pl,t+\Delta t}\,\mathbf{M}_{\Delta pl}.\end{aligned} \tag{3}$$

The corresponding exposure centers are

$$\begin{aligned}\mathbf{r}_{Io} &= (X_o,Y_o,Z_o)_t \\ \mathbf{r}_{IIo} &= (X_o,Y_o,Z_o)_{t+\Delta t} + \mathbf{M}_{II,t+\Delta t}\,\Delta\mathbf{r}.\end{aligned} \tag{4}$$

The baseline is the difference between $\mathbf{r}_{IIo}$ and $\mathbf{r}_{Io}$: i.e.,

$$\mathbf{B} = \mathbf{r}_{IIo} - \mathbf{r}_{Io}. \tag{5}$$

A coplanarity equation can be established by requiring that the three vectors, i.e., $\mathbf{B}$, $\mathbf{r}_I$, and $\mathbf{r}_{II}$, be on the same plane: i.e.,

$$\mathbf{B}\cdot(\mathbf{r}_I \times \mathbf{r}_{II}) = 0. \tag{6}$$

$\mathbf{r}_{II}$ and $\mathbf{r}_I$ are expressed as

$$\begin{aligned}\mathbf{r}_I &= -\lambda_I\,\mathbf{M}_{I,t}\,(x_I,0,f_I)^T, \\ \mathbf{r}_{II} &= -\lambda_{II}\,\mathbf{M}_{II,t+\Delta t}\,(x_{II},0,f_{II})^T.\end{aligned} \tag{7}$$

Equation 7 is then inserted into Equation 6. With known baseline $\mathbf{B}$, known interior and exterior orientation parameters (f_I, f_{II}, $\mathbf{M}_{I,t}$, $\mathbf{M}_{II,t+\Delta t}$), and measured image coordinates (x_I and x_{II}) of the object point P, the two scaling factors λ_I and λ_{II} are solved for by a least-squares adjustment of the equations resulting from Equation 6. Using the calculated λ_I and λ_{II} in Equation 7, $\mathbf{r}_I$ and $\mathbf{r}_{II}$ become known. Finally, the position of point P or $\mathbf{r}$ = (X,Y,Z) can be computed by either of the following equations:

$$\begin{aligned}\mathbf{r} &= \mathbf{r}_{Io} + \mathbf{r}_I \text{ or} \\ \mathbf{r} &= \mathbf{r}_{IIo} + \mathbf{r}_{II}.\end{aligned} \tag{8}$$

Navigation Data as Exterior Orientation Parameters

In Equations 1 through 8, both interior and exterior orientation parameters are assumed to be known. The imaging platform positions of $(X_o,Y_o,Z_o)_t$ and $(X_o,Y_o,Z_o)_{t+\Delta t}$ at time t and $t+\Delta t$ are measured by onboard kinematic DGPS (Differential Global Positioning System) to an accuracy of 3 m. The corresponding rotation angles of the imaging platform $(\omega, \phi, \kappa)_{pl,t}$ and $(\omega, \phi, \kappa)_{pl,t+\Delta t}$ ($\mathbf{M}_{I,t}$ and $\mathbf{M}_{I,t+\Delta t}$) are determined by star trackers to an accuracy of two arcseconds. In fact, the sampling rates of DGPS and star trackers are usually lower than that of image recording. DGPS and startracker data are not available for every image line. There will be polynomial interpolations of navigation data between "orientation lines" which are image lines with actual DGPS and startracker navigation data. Such interpolations can also be performed using orbital parameters (Slama *et al.*, 1980). The interpolated navigation data along with the imagery can be distributed to users. On the other hand, the polynomial interpolation parameters can be estimated through a bundle adjustment procedure using ground control points (GCP), as applied in airborne or space shuttle "three-line" photogrammetric mapping (Hofmann, 1986; Heipke *et al.*, 1996). The satellite orbit is assumed to be relatively smooth, so that the need for high-order polynomial interpolations is not anticipated. An appropriate interpolation model in a bundle adjustment should be determined by experimentation using real data. In addition,

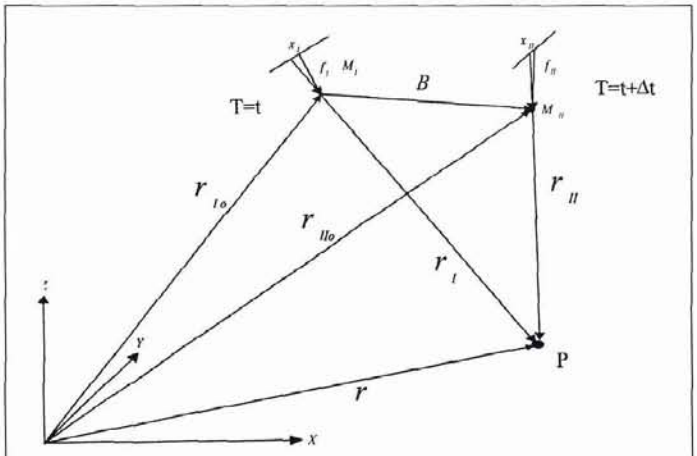

Figure 4. Photogrammetric intersection in in-track stereo mode.

DGPS and startracker navigation data can be treated as "non-perfect" position and attitude observations. The least-squares adjustment will make corrections to these observations depending on weights (confidences) assigned accordingly.

Although IKONOS I will be implemented with only one CCD linear array instead of three, it will be preprogrammed to point to the mapping area in order to build the fore-looking strip when approaching the area; the imaging system changes its pointing angle and aims downward to generate the nadir-looking strip; the aft-looking strip is taken in the same way (Parker, 1997). The *stereo* strips will have a limited length. However, they will satisfy many applications and will be complemented by its cross-track stereo option. The above discussed model fits IKONOS I stereo imagery also.

Potential for National Mapping Products

Error Estimation

According to the technical specifications of the satellite imaging companies, positional accuracies of objects derived from high-resolution satellite imagery are 12 m (horizontal) and 8 m (vertical) without GCPs, and 2 m (horizontal) and 3 m (vertical) with GCPs (Fritz, 1996). An independent estimation of the accuracies is given using certain assumptions and error propagations. Errors of exposure centers provided by DGPS are $\sigma_{xo} = \sigma_{yo} = \sigma_{zo} = 3$m. Errors of the platform attitude from startrackers are $\sigma_{\omega o} = \sigma_{\phi o} = \sigma_{\kappa o} = 2$ arcseconds. The elevation error of a ground point derived from a vertical stereo photograph pair caused by flying height error σ_H, baseline errors σ_B, and image parallax measurement error σ_p can be estimated as (Wolf, 1983)

$$\sigma_{h1}^2 = \sigma_H^2 + [(H-h)/B]^2\sigma_B^2 + (H-h)^4/[B^2f^2]^2\sigma_p^2. \tag{9}$$

Considering relationships between the exposure centers, the flying height, and the baseline, σ_H and σ_B are evaluated as $\sigma_{zo} = 3$m and $1.414\sigma_{xo} = 4.24$m, respectively. An image coordinate measurement error of 0.5 pixels (6 μm) is assumed. The parallax measurement error σ_p is then 8.5 μm. In Equation 9, let $(H - h) = H = 680$km, $f = 10$m, and $B = 680$km (F-N or N-A stereo). σ_{h1} is evaluated as $\sigma_{h1} = [9\text{m}^2 + 18\text{m}^2 + 0.3\text{m}^2]^{1/2} = 5.2$m. Note that σ_{h1} considers the impact of positional DGPS navigation errors implicitly through σ_H and σ_B. Ideally, the attitude error of the nadir-looking linear array does not contribute to the elevation error of the ground point. The contribution by the fore or aft linear array is

$$\sigma_{h2} = H\,\sigma_\omega = 6.6\text{ m}. \tag{10}$$

The overall elevation error of the point without GCPs is $\sigma_h = (\sigma_{h1}^2 + \sigma_{h2}^2)^{1/2} = 8.4$m, which is close to the specified error of 8 m by the imaging companies. In the same way, the horizontal error (without GCPs) of 13.2 m can be derived under the same assumptions, compared to 12 m specified by the imaging companies.

It should be noted that the above error estimation does not take into account the effect of the interpolation of navigation data. This effect can only be determined effectively when actual data are available after the successful launch of the satellites. Furthermore, the specified accuracies of ground points with GCPs are also difficult to verify without actual data. Ridley *et al.* (1997) simulated the 1-m resolution data from 0.2-m resolution aerial photographs. Using the geometry of frame cameras instead of CCD linear arrays, the ground point error was around 2m (with GCPs). Airborne three-line scanner imagery of 2 m resolution with GCPs demonstrated a ground accuracy of 1 m (horizontal) and 2 m (vertical) (Heipke *et al.*, 1996). A bundle adjustment combines interpolation parameters of navigation data, image measurements, navigation measurements, and unknown coordinates of the measured ground points in a strict mathematical model and is capable of providing a better ground point accuracy under global optimal conditions. Specific issues such as distribution of GCPs, minimum number of GCPs for each national mapping product, and correlations between parameters of the bundle adjustment need to be addressed based on experiments using actual data.

Application Potential for DEM, DOQ, and DLG

Although hard copies of 1:24,000-scale topographic maps have been scanned and/or digitized for producing digital national mapping products of DEMs, DOQs, and DLGs, aerial photographs are the primary data used to derive information necessary for the products. These photographs usually have a base-height ratio of 0.63. This requirement can be met easily by forming stereo pairs using F-N and N-A combinations. Elevation error σ_h in a DEM is required to be less than 15 m. This requirement can be met without GCPs. DOQ and DOQQ (Digital Orthophoto Quarter-Quadrangles) products have a resolution of 2 m to 1 m, respectively. Elevation errors of a DEM needed to produce DOQ are required to be less than 7 m. The image resolution requirement is met. The elevation error of less than 7 m can only be satisfied by applying GCPs according to the above analysis. DLG (1:24,000 scale) allows the horizontal error to be smaller than 12 m and the vertical error smaller than 15 m. The required elevation error of 15 m is greater than the estimated elevation error without GCPs. Although the required horizontal error of 12 m equals the specified horizontal error (without GCPs), it is recommended that GCPs be used.

In addition to geometric accuracy, the capability of representation of topographic objects and extraction of the information from the imagery is of great interest. The 1-m resolution stereo imagery of the panchromatic band should be able to give sufficient image features for the generation of DEM grid points spaced every 30 m manually or automatically by digital image matching techniques. Existing DEMs that may be updated using such imagery can be employed to produce black-and-white DOQQs of 1 m resolution (3.75-minute quarter-quadrants) and DOQs of 2-m resolution (7.5-minute quadrangles). Additional 4-m resolution multispectral DOQs may be produced as byproducts using the multispectral bands and the same DEMs. Attributes of 1:24,000-scale DLG quadrants are derived from maps of the same scale (USGS, 1997). Their base categories include (1) political boundaries, (2) hydrography, (3) Public Land Survey System (PLSS) data, (4) transportation data, (5) other significant manmade structures, (6) hypsography, (7) surface cover (e.g., vegetative surface cover), (8) nonvegetative surface features (e.g., lava and sand), and (9) surface control and marks. Categories (3) and (9) are usually well documented by relevant federal agencies. Their update in the DLG quadrants can be performed either manually or automatically. The information update of the rest of the categories can be, in principle, carried out by using high-resolution satellite imagery. Positive results of attribute information extraction from simulated high-resolution satellite imagery for the Ordnance Survey of the UK were reported (Ridley, 1997). Experiments using actual data should be performed to verify the capability for DLG quadrants.

Application Potential for DSL

Theoretically, an instantaneous shoreline is the intersecting line between a Coastal Terrain Model (CTM), which is a digital surface model of a strip of land along the shoreline with onshore elevation and nearshore bathymetry, and a water surface. It changes as the water surface increases or decreases. Therefore, a tide coordinated shoreline should be defined based on a certain water datum. The National Geodetic Survey (NGS) of NOAA (National Oceanic and Atmospheric Administration) produces the nation's tide coordinated Mean Lower-Low Water (MLLW) and Mean High Water (MHW) shorelines in nautical charts. These datums refer to the synoptic averages over a 19.2-year lunar/solar cycle. NGS derives the tide-coordinated shorelines using periodic aerial photographs taken at the time of the desired water level using coordinated quasi real-time hydrographic observations (Slama *et al.*, 1980). Because a satellite has a prescribed orbit, there is no control over imaging the coast area at the time of the desired water level. The satellite has a revisit rate of 1 to 4 days. The CTM may change along with time because of erosion, land use, and other natural or human activities in the coastal zone. The instantaneous shorelines thus derived from the high-resolution satellite imagery vary according to both the CTM and water level.

The stereo satellite image strips can be used to determine the CTM. Onshore land elevations of grid points of the CTM are computed by either image matching or interactive measurements on panchromatic images. Offshore grid points within the shallow area may be determined in the same way from multispectral band images (4-metre resolution), which penetrate water better than visible band images (Slama *et al.*, 1980; Lillesand and Kiefer, 1994). Within a time period, a set of low-water satellite images can be accumulated and used to generate a reliable CTM with a maximum number of grid points determined from high-resolution panchromatic images. This CTM can be used wherever no instantaneous CTM is necessary. The accuracy of the CTM is expected to be 2m horizontal and 3 m vertical with GCPs. Water surface levels can be modeled by a computer modeling system using tide-gauge observations and other hydrographic data along the shoreline. A water surface model may have a vertical accuracy of several centimetres (Bedford and Schwab, 1994). Because historical water level data have been archived, both MLLW and MHW can be determined.

The instantaneous shoreline at the time of imaging is projected in the image strips. This line separates the land and water areas and can be extracted either interactively by on-screen digitizing or automatically by edge enhancement and edge following. The position of the shoreline in the ground coordinate system is triangulated from the extracted lines in stereo strips. The instantaneous shorelines derived from the satellite imagery at different times should be corrected to tide-coordinated shorelines. Data used for this correction include the instantaneous shorelines, updated CTM, and the instantaneous water level and desired water datum. Research on the correction algorithms should be conducted to make the comparison of the shorelines and the estimation of a datum coordinated shoreline possible.

The Digital Shoreline (DSL) is calculated from shorelines generated periodically over a long term. Currently, the National Geographic Data Committee is preparing a National Standard for Digital Shoreline Databases (NGDC, 1997). It is expected that the accuracy of CTM grid points will be 2 to 3m. The water level accuracy is to submetres. Consequently, the DSL generated using the above method should have the potential to produce DSL. An extreme case would be a very flat coastal area where a small vertical error would yield a large horizontal error of the shoreline. Such a difficulty should be overcome by examining both the estimated shoreline and the shorelines in images.

Discussions and Conclusions

The estimation and analysis presented above show a great potential of the upcoming high-resolution satellite imagery for national mapping products. Verification of the potential and assessment of the general mapping capabilities of the imagery are envisioned by The Ohio State University. A high altitude aerial photogrammetric calibration range in Madison County, Ohio will be used for DEM, DOQ, and DLG related experiments. The range consists of approximately 23 ground control points (GCPs) located within a rectangular region of 14 miles east to west and 9 miles north to south. The range center is at about latitude 39°56'24" N and longitude 83°24'42" W (NAD-83). The GCPs are distributed mostly in an east-west direction. One of the lines (US 40) has GCPs in an east-west extent of 13 to 15 km, which gives cross-track control of satellite images. The targets consist of painted circles on asphalt pavement. Each has a 1-metre circle, centered on the monument and painted flat white. A 3-metre flat black circle is painted as background to enhance the contrast. The range was surveyed by GPS methods, and a network adjustment was applied. All targets along US 40 are known in WGS84 based on a second-order station at the Madison County Airport. They are internally consistent in three dimensions to about 2 cm RMSE. The target points are distributed in three zones. Zone I covers mostly rural and agricultural objects, Zone II is a part of the highway, and Zone III covers more manmade objects, such as buildings, roads, and parcels. Because the range does not provide significant elevation variation, an additional site will be needed for a DEM experiment. An experiment of DSL is to be carried out for the shoreline segment of Lake Erie. Shorelines derived from periodic satellite imaging observations will be used for monitoring shoreline changes from erosion. Causes and impact of shoreline erosion can be analyzed by integration of the shoreline changes and other scientific and social economic data in a GIS environment (Li and Cho, 1996).

A number of technical aspects will have to be dealt with for mapping purposes. They include, among others,

- Increased impact of atmospheric refraction and Earth curvature,
- Development/improvement of photogrammetric CCD linear array models, and
- Overcoming low visibility caused by cloud cover in certain areas.

The third aspect may be considered along with applications of other satellite data which are less weather dependent, such as RADARSAT, to achieve so-called all-weather mapping capability. This is especially important when dealing with event-based mapping, for instance, shoreline monitoring and flood mapping.

It is expected that high-resolution satellite imagery can be, to some extent, used to reduce the demand for aerial photographs for middle scale to some large-scale (for example, 1:24,000) mapping. Strict photogrammetric models will be employed to derive accurate horizontal and vertical position information from the imagery. Additional characteristics of the imagery such as periodic and global coverage, strong spectral capability, and Internet based ordering and distribution systems make the technology even more attractive to the mapping community. Overall, high-resolution satellite imagery will mark a significant advancement of applications of satellite imaging technology in mapping.

Acknowledgments

Discussions on technical and relevant issues with M. Lockwood, L. Lapine, G. Leigh, N. Schmidt, C. Fowler, S. Mackey, K. Bedford, and D. Roberts are appreciated. The DSL related research is currently supported by a Grant from Sea Grant — NOAA Partnership Program and CSC, NGS, and OCS of NOAA. Comments from reviewers are appreciated.

References

Al-Rousan, N., P. Cheng, G. Petrie, T. Toutin, and M.J.V. Zoej, 1997. Automated DEM Extraction and Orthoimage Generation from SPOT Level 1B Imagery, *Photogrammetric Engineering & Remote Sensing*, 63(8):965–974.

Bedford, K., and D. Schwab, 1994. The Great Lakes Forecasting System - An Overview, *Proceedings of National Conference on Hydraulic Engineering*, 1-5 August, Buffalo, N.Y., pp.197–201.

Ellis, M.Y., 1978. *Coastal Mapping Handbook*, USGS/NOS Publication.

FGDC, 1997. Public Comment on the Proposal to Develop the "National Shoreline Data Standard" as a Federal Geographic Data Committee Standard, *Federal Register*, 62(156):43342–43344.

Fraser, C., P. Collier, J. Shao, and D. Fritsch, 1997. Ground Point Determination Using MOMS-02 Earth Observation Imagery, *Geomatica*, 51(1):60–67.

Fritz, L.W., 1996. Commercial Earth Observation Satellites, *Intl. Archives of Photogrammetry and Remote Sensing*, ISPRS Com.IV, pp. 273–282.

Heipke, C., W. Kornus, and A. Pfannenstein, 1996. The Evaluation of MEOSS Airborne Three-Line Scanner Imagery: Processing Chain and Results, *Photogrammetric Engineering & Remote Sensing*, 62(3):293–299.

Hofmann, O., 1986. Dynamische Photogrammetrie, *Bildmessung und Luftbildwesen*, 54(3):105–121.

Li, R., 1997. Mobile Mapping: An Emerging Technology for Spatial Data Acquisition, *Photogrammetric Engineering & Remote Sensing*, 63(9):1085–1092.

Li, R., and W.K. Cho, 1996. Geographical Information Systems for Shoreline Management - A Malaysian Experience, *Proceedings of ADB Coastal Erosion Conference*, Kuala Lumpur, Malaysia, 9 p.

Li, R., K.P. Schwarz, M.A. Chapman, and M. Gravel, 1994. Integrate GPS, INS, and CCD Cameras for Rapid GIS Data Acquisition, *GIS World*, 7(4):41–43.

Lillesand, T.M., and R.W. Kiefer, 1994. *Remote Sensing and Image Interpretation*, John Wiley & Sons, Inc.

Lockwood, M., 1997. *NSDI Shoreline Briefing to the FGDC Coordination Group*, 7 January 1997, NOAA/NOS (unpublished), 29 p.

Moffitt, F.H., and E.M. Mikhail, 1980. *Photogrammetry*, Harper & Row Publishers, Inc., New York, N.Y.

Parker, J.L., 1997. The Advantages of In-Track Stereo Acquisition from High-Resolutin Earth Resource Satellites, *Proceedings of 1997 ACSM/ASPRS Annual Convention & Exposition*, pp. 276–282.

Ridley, H.M., P.M. Arkinson, P. Aplin, J.-P. Muller, and I. Dowman, 1997. Evaluating the Potential of the Forthcoming Commercial U.S. High-Resolution Satellite Sensor Imagery at the Ordnance Survey, *Photogrammetric Engineering & Remote Sensing*, 63(8): 997–1005.

Slama, C.C, C. Theurer, and S.W. Henriksen (editors), 1980. *Manual of Photogrammetry*, American Society of Photogrammetry, Falls Church, Virginia.

USGS, 1997. *Fact Sheets and WWW Pages of GeoData: Digital Line Graphs, Digital Elevation Models, and Digital Orthophotos*, U.S. Geological Survey, Reston, Virginia.

Wolf, P.R., 1983. *Elements of Photogrammetry*, McGraw-Hill, Inc.

(Received 03 September 1997; accepted 24 February 1998; revised 10 March 1998)